RF-based Stent-Graft Endoleakage Monitoring System

Cristina Oliveira*, Nuno Almeida‡ and José Machado da Silva*
*INESC TEC, Faculdade de Engenharia, Universidade do Porto, Portugal
Email: {cristina.oliveira,jms}@fe.up.pt
‡Faculdade de Engenharia, Universidade do Porto, Portugal
Email: nunocmalmeida@gmail.com

***Abstract*—A monitoring system to detect endoleaks in patients that undergo an EVAR procedure is presented which avoids the need for more complex biomedical imaging systems. The system resorts to capacitive pressure sensors placed in the stent-graft and monitored externally by means of an inductive coupling with the purpose of measuring the oscillation frequency of the LC resonant circuit created by the capacitive sensor and the inductor. Experimental results show that reliable measurements can be obtained with a power level well below that established to prevent damaging of living tissues.**

***Resumo*—É apresentado um sistema de monitorização de fugas em próteses endovasculares implantadas em pacientes submetidos a uma intervenção de reparação do aneurisma na aorta, que evita a necessidade de realização de exames imagiológicos mais complexos. Essas fugas são detetadas a partir da sensorização de pressão na prótese endovascular por intermédio de acoplamento inductivo que permite medir a frequência de oscilação do circuito LC ressonante formado pelo sensor e a inductância. Os resultados experimentais obtidos evidenciam que podem ser realizadas medições fiáveis com um nível de potência inferior àquele estabelecido para evitar danos nos tecidos humanos.**

***Index Terms*—inductive-coupling, telemetry, endoleaks, pressure sensor.**

I. Introduction

An abdominal aortic aneurysm (AAA) is a ballooning of the abdominal aorta, currently one of the most common causes of death in the western world [1]. The current available treatments are the open surgery and the endovascular aneurysm repair (EVAR). The last one is a minimally invasive procedure in which a stent-graft is inserted in the affected artery segment to prevent wall rupture, shielding the aneurysm from the blood pressure. Although EVAR is preferable due to the lower morbidity and mortality rate, anomalies can occur after the stent-graft placing, namely endoleaks [2]. Post-EVAR monitoring within intervals of 6 months to one year is therefore of utmost importance, in order to avoid AAA rupture and the need for reinterventions [3].

One of the most important parameters to be measured is the intra-sac/stent-graft pressure, whose deviation reveals the presence of the previously mentioned complications. Current monitoring procedures are performed using medical imaging modalities, but these present several drawbacks, namely cost and the lack of actual pressure measurements. To overcome these limitations, remote monitoring systems have been proposed, such as the EndoSure Sensor (CardioMEMS, Atlanta, GA, USA) and the ImPressure Sensor (Remon Medical Technologies, Caesarea, Israel) [4] which have already been tested in clinical trials, showing good results [5]. The first uses a resonant circuit delivered into the aneurysm sac during the EVAR intervention, and a complex antenna and receiver circuit. Even though it provides good results, its implantation adds complexity to the EVAR procedure, there is no control over its exact position and it occupies much space in the sac, allowing the placement of a single sensor [6]. By its turn, the ImPressure Sensor is hand sewed to the outside of the stent-graft and is activated by ultrasound waves using a hand-held probe. Despite the safety of using ultrasound for medical purposes, the waves do not propagate through air or bone, which may lead to difficulties in communicating with the aneurysm sac.

A. Remote Monitoring System

The authors of this paper have presented an alternative solution consisting of a small and flexible sensor that may be integrated in the stent-graft [7]. This sensor shows the advantage of being possible to be collapsed together with the stent-graft without damage, and is thus implanted without the need for different or additional procedures. Moreover, the design is very simple, it uses the same frequencies for powering and communication and permits monitoring a cluster of sensors disposed along the stent-graft with a single external reader. It is thus possible to obtain a profile of the stent pressure, improving the reliability of the monitoring process.

Each single sensor consists of an LC parallel resonant circuit with a simple transduction principle. While the inductance is fixed, the capacitance is obtained with two plates with air as the dielectric. When the pressure changes so does the distance between the plates and therefore the capacitance. Upon stimulation with an electromagnetic field from the external reader circuit, the resonant circuit oscillates at its natural resonance frequency, which is a function of sensor's L and C.

The inductor is implemented with a flexible print circuit board (PCB), consisting on a planar inductor of copper deposited over a flexible substrate of polyimide with 50 μm of thickness. Each capacitor plate is made of a $\sim$50 μm thickness polydimethylsiloxane (PDMS) and carbon nanotubes (CNTs) substrate with a very thin gold deposition. The capacitor plates are soldered to the inductor contacts in the coil center, where

a gap is left with air (dielectric). The whole sensor (inductor + capacitor) is then encapsulated with a PDMS cover to ensure biocompatibility. Dimensions go from 10x10 to 20x20 mm^2 area and $\sim$220 μm thickness. The oscillation frequency seen at the receiver inductor depends only on the sensor elements and the coupling factor (k), as reported in [8] according to the following equation:

$$f_{osc} = \frac{1}{2\pi\sqrt{(1-k^2)L_s C_s}} \quad (1)$$

The remote energizing and reading principle is based on inductive coupling, using an inductor outside the human body as antenna. A transient in the primary inductor (antenna) generates a damped oscillation which is then amplified and converted to digital at the reading circuit [7]. Stimulation is provided by means of a square wave whose frequency (100 kHz) is chosen in order to accommodate the typical duration of the oscillation before it is fully damped ($\sim$5 us).

B. Wireless Biomedical Communication

The RF (radio-frequency) wave propagation in a biological medium is very different from that occurring in classic communications systems. Since the electromagnetic wave is passing through different media that have vastly different electrical properties, the propagation speed is significantly reduced in some organs and may induce significant time dispersion that varies with each organ and tissue layer. When powering implanted devices via inductive coupling, most of the power loss is due to electromagnetic wave reflection at the skin-air interfaces and heat dissipation in the tissues. Taking into account that the electromagnetic waves at the resonant frequency travel through blood, blood vessel, muscle, fat and skin tissues before reaching the outside, properties of those tissues must be taken into account for the choice of frequencies of work. Figure 1 shows the penetration depth of RF waves for different biological tissues.

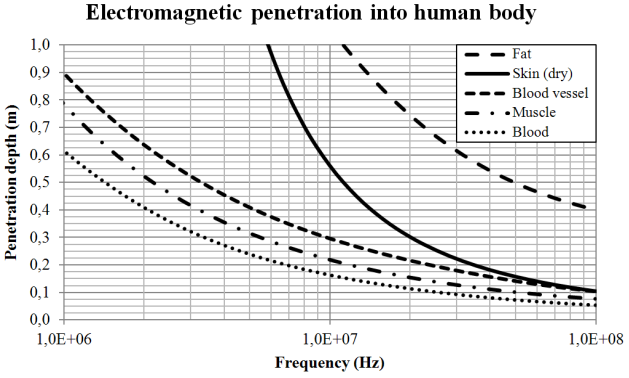

Figure 1: Penetration depth of electromagnetic waves in the 1MHz - 100MHz range, for different types of biological tissues [9].

As far as communication efficiency (efficient power transfer) is concerned, penetration depth is extremely important to ensure that the electromagnetic waves travel all the distance between the inductors. Good electromagnetic permittivity is closely related and is essential to ensure an efficient power transfer. As working distances are in the order of $\sim$5 cm, frequencies above 50 MHz should be avoided, giving preference to those below 20 MHz (15 to 20 cm penetration depth ensured). This also guarantees operation in the antennas near-field [10], where the electromagnetic induction is more efficient. In what concerns to protection of the biologic tissues, heat dissipation must be minimized. As tissues' conductivities increase at higher frequencies, this is achieved for lower frequencies. However, frequencies below the MHz range would require larger LC components for the antenna and sensor. In addition, the quality factor of the inductive coupling decreases at low RF frequencies, due to losses in the tissues [11].

For the aforementioned reasons, the 12.5 MHz to 20 MHz range is used, and the sensor L and C values are designed to resonate in this frequency range. Actually, these frequencies are in the ranges allocated for industrial, medical implants communications and scientific applications [12]. Frequency range extension may be considered (below 50 MHz) if extra-bandwidth becomes necessary to accommodate a sensor cluster, depending on the number of sensors.

C. Biological concerns

An important issue when building a system that relies on inductive coupling to communicate with an implantable sensor, is the level of energy absorbed by the body, leading to an increase of temperature and eventually damage the living cells and tissues. The specific energy absorption rate (SAR) is used as a standard parameter to quantify heating generated by magnetic and electrical fields in biological tissue and is included in the legislation for electronic devices such has cell phones and MRI equipment.

$$SAR = \frac{\sigma E^2}{2\rho} \quad (2)$$

The SAR is mainly dependent on the incident electrical field (E) and is also related to the tissue electrical conductivity (σ) and density (ρ). According to the European directive 1999/519/EC the averaged SAR during a period of 6 minutes should not exceed 0.08 W/kg for frequencies between 10 MHz and 10 GHz. This directive also includes limits for maximum permissible exposure (MPE) regarding E-field strength (28 V/m), H-field strength (0,073 A/m), B-field (0,092 μT), and the equivalent plane wave power density S_{eq} (2 W/m^2) [13].

The IEEE Standard for Safety Levels with Respect to Human Exposure to Radio Frequency Electromagnetic Fields, 3 kHz to 300 GHz (IEEE Std C95.1), specifies that levels of energy (maximum peak energy level) at 100 kHz, with a passive antenna (inductor) next to the chest result in exposures of $\sim$0.051 mW/cm^2, i.e., $\sim$0.05% of the MPE limit for controlled environments.

II. Telemetry System

The previously described telemetry system has been developed in order to remotely and easily read the pressure

values of the implantable sensor. The prototype conceived as a demonstrator of external reading system comprises a generator of the square wave applied at the terminals of the primary inductor (Reader), a transformer (TF) to subtract the common-mode from the signal received by the inductor and amplify the oscillation frequency, instrumentation amplifiers (IA) and filters (LPF) to improve the signal-to-noise ratio (SNR) and set the signal ready for optimum A/D conversion. The signal is then acquired at 250 Msps and post-processed to improve the oscillation frequency detection. Post-processing includes detection, segmentation and averaging of multiple cycles to reduce noise, application of a Hanning window to compensate for non-coherent sampling. Finally a fast Fourier transform (FFT) is applied to detect the oscillation frequency. Figure 2 synthesizes the described system, which is described in detail in [7].

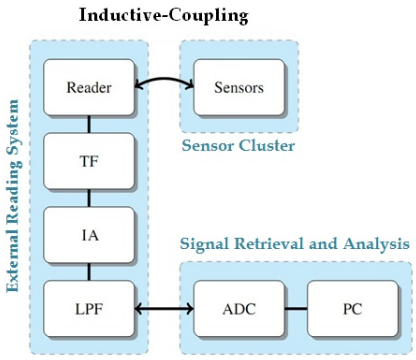

Figure 2: Blocks diagram of the telemetry system. TF - transformer; IA - instrumentation amplifier; LPF - low pass filter; ADC - analog to digital converter; PC - personal computer.

To test the capability of the system to detect changes in the sensor capacitance, a model of the sensor was implemented in PCB consisting of a LCR resonator with a square planar inductor (L_S = 10.8 μ H), a replaceable capacitor (C_S) and a resistor (R_S = 12 Ω). Experiments were performed with different capacitances in the sensor model. The oscillation frequencies detected in each case are shown in Table I. The expected values obtained with equation 1 are also presented. The differences observed between the expected and measured values reveal that the theoretical expression may not completely model the system due to, namely, parasitic elements that bring complexity in the theoretical model. Nevertheless, the oscillation frequency can be unequivocally measured as a function of the sensor capacitance. Considering a calibration step that provides the f-vs-C_S characteristic, any further variation in the capacitance (as function of blood pressure) can be detected and measured with this telemetry approach.

After the analog subtraction of the reference signal, amplification of the resonance frequency, and filtering the signal shows a good SNR. At typical distances the SNR is 27 dB (1.5 cm) down to 3.4 dB (4.5 cm). However, the described signal processing operations improve this to 45.6±8.4 dB in the same range of distances. Figure 3 shows the aspect of the transient after processing.

Table I: Experimental and theoretical values of the oscillation frequencies detected for different sensor capacitances.

C_S (pF)	detected f_{osc} (MHz)	theoretical f_{osc} (MHz)
7.3	15.09	18.03
8.3	14.60	16.90
9.2	14.27	16.01
10.2	13.69	15.21
14.1	12.22	12.94
15.1	12.07	12.51

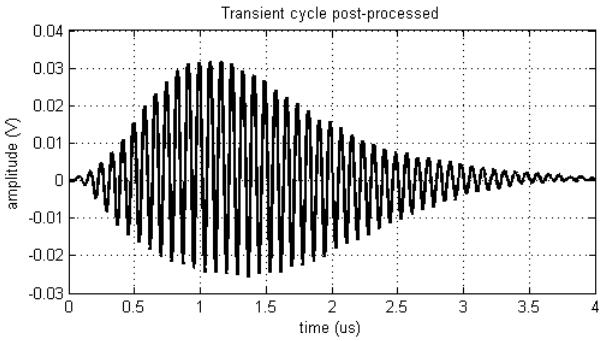

Figure 3: Example of the transient signal after Hanning windowing and cycle-averaging operations (C_S = 15.1 pF, detected frequency = 12.07 MHz).

In order to evaluate the reliability of each reading, frequency domain parameters are calculated with respect to the main lobe around the fundamental frequency (see figure 4). In addition to the SNR, the spurious-free dynamic range (SFDR) is calculated. Ideally, in a real-life situation, the controller should repeat the sampling process until a good measurement is achieved (high SFDR and SNR).

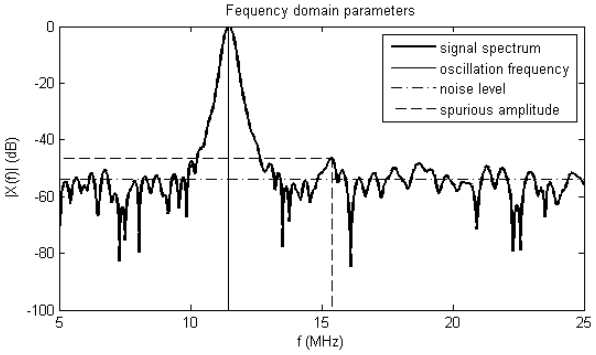

Figure 4: Spectrum of frequencies of the post-processed signal, showing the detected frequency and the corresponding SNR and SFDR parameters.

III. Energy and Biological Considerations

With the sensor inside the human body, when reading from the outside it is also necessary to account for the effect of the biological tissues. Permeability to electromagnetic radiation (particularly in RF) in this medium is lower than in the air.

Also, tissue-tissue and tissue-air interfaces affect the energy transmission and so the inductive coupling. Experiments with a tissue-emulating phantom (recipes from [14]) show that the detected frequency decreases about 4 MHz in biological medium. Moreover, these experiments show that the inductive coupling is degraded when the sensor is inside the human body, attenuating the SNR about -11dB. With the post signal processing this degradation is less severe, as SNR is reduced from $\sim$45 dB to $\sim$34 dB (28 dB in the worst case) which is still a very good level.

The referred readout values were obtained at very low power levels. The transmitted power is in the order of 4.9 mW root-mean-squared (RMS) and 43 mW at its peak. These values are well bellow the IEEE Standard for Safety Levels with Respect to Human Exposure to Radio Frequency Electromagnetic Fields, showing that good and reliable measurements are achieved without any risk for the patient in terms of exposure to electromagnetic radiation.

The resonance of the LC sensor (absorbed energy) occurs at power levels of 19 μW RMS (2.4 mW peak). This represents a very low efficiency of 0.4%, which is expectable in inductive coupling systems. Regardless of the small fraction of emitted energy that is converted to actual valuable signal, the reading system is able to detect it with very good accuracy and reliability. This shows that the low energy efficiency is not a problem, enhancing the fact that the inductive coupling brings ease-of-design to the circuit, without compromising the telemetry between the implanted sensor and the outside world.

Simulations were performed with the SEMCAD® software, using models of the antennas specifically designed to match those used in this system, as well as medium properties similar to the human tissues. SAR was calculated and compared to the safety limits. The software applied the finite-difference time-domain algorithm (FDTD) [15] estimating SAR values of 0.0136 W/kg (averaged over 6 minutes, as stated by the legislation), which is significantly lower (17%) than the specified limit (maximum $SAR_{AVERAGE}$ = 0.08 W/kg).

IV. Conclusions

A telemetry system for monitoring the status of aortic stent-grafts is being developed. Simulation and experimental results indicate that the system provides a good solution to detect pressure variations (with capacitive sensors) caused, e.g. by of endoleaks, by means of a simple magnetic coupling. Experimental results obtained with demonstration prototype boards implementing the external reading system, showed that the induced voltage in the sensor was lower than the limit that would be imposed by legislation. Also, simulations performed for the SAR estimation indicate that heating generated in the living tissues due to the magnetic coupling is below the permitted levels.

Acknowledgments

This work has been carried-out in the framework of project EDAM-SenseCardioHealth with the support of programme MIT|Portugal, Fundação para a Ciência e a Tecnologia, grant MIT-Pt/EDAM-EMD/0007/2008 and grant contract SFRH/BD/81476/2011.

References

[1] S. Murphy, J. Xu, and K. Kochanek, "Deaths: Preliminary data for 2010," *National Vital Statistics Reports*, vol. 60, no. 4, p. 68, 2012.

[2] T. Chuter, J. Parodi, and M. Lawrence-Brown, "Management of abdominal aortic aneurysm: a decade of progress," *Journal of Endovascular Therapy*, vol. 11, no. II, pp. II82–II95, 2012.

[3] B. T. Katzen and A. A. MacLean, "Complications of endovascular repair of abdominal aortic aneurysms: A review," *CardioVascular and Interventional Radiology*, vol. 29, pp. 935–946, 2006.

[4] R. Milner, K. Kasirajan, and E. L. Chaikof, "Future of endograft surveillance," *Seminars in Vascular Surgery*, vol. 19, no. 2, pp. 75 – 82, 2006.

[5] C. J. Parsa, M. A. Daneshmand, B. Lima, K. Balsara, R. L. McCann, and G. C. Hughes, "Utility of remote wireless pressure sensing for endovascular leak detection after endovascular thoracic aneurysm repair," *The Annals of Thoracic Surgery*, vol. 89, no. 2, pp. 446 – 452, 2010.

[6] F. Springer, R. W. Günther, and T. Schmitz-Rode, "Aneurysm Sac Pressure Measurement with Minimally Invasive Implantable Pressure Sensors: An Alternative to Current Surveillance Regimes after EVAR?" *Cardiovasc Intervent Radiol*, vol. 31, no. 3, pp. 460–467, 2008.

[7] C. Oliveira, N. Almeida, and J. Machado da Silva, "Inductive coupling system for endovascular aneurysm repair monitoring," *Studies in health technology and informatics*, vol. 177, pp. 101–6, 2012.

[8] A. Moreira, J. M. da Silva, and L. A. Rocha, "Endoleakage monitoring using inductive-coupling," *XXV Conference on Design of Circuits and Integrated Systems (DCIS'2010)*, November 2010.

[9] C.Gabriel, "Compilation of the dielectric properties of body tissues at rf and microwave frequencies," *Technical reports, Brooks Air Force*, no. AL/OE-TR-1996-0037, 1996.

[10] K. Fotopoulou and B. Flynn, "Wireless powering of implanted sensors using RF inductive coupling," *Proceedings of IEEE Sensors*, pp. 765–768, 2006.

[11] U. Jow and M. Ghovanloo, "Modeling and optimization of printed spiral coils in air, saline, and muscle tissue environments," *IEEE Transactions on Biomedical Circuits and Systems*, vol. 3, no. 5, October 2009.

[12] "The European table of frequency allocations and utilizations in the frequency range 9 KHz to 3000 GHz," Electronic Communications Commitee (ECC), Tech. Rep., 2009.

[13] 1999/519/EC, "Council recommendation of 12 july 1999 on the limitation of exposure of the general public to electromagnetic fields (0 Hz to 300 GHz)," *Official Journal of the European Communities*, no. L 199, pp. 59–70, July 1999.

[14] G. Hartsgrove, A. Kraszewski, and A. Surowiec, "Simulated biological materials for electromagnetic radiation absorption studies," *Bioelectromagnetics*, vol. 8, no. 1, pp. 29–36, 1987.

[15] SEMCAD X, "Reference manual for the semcad simulation platform for electromagnetic compatibility, antenna design and dosimetry," *SPEAG - Schmid & Partner Engineering, AG*, 2012.